



Molecular Crystals and Liquid Crystals Science and Technology. Section A. Molecular Crystals and Liquid Crystals

Publication details, including instructions for authors and
subscription information:

<http://www.tandfonline.com/loi/gmcl19>

STM Tip Induced Phase Transition of Copper Tetracyanoquinodimethane (CuTCNQ)

Shoji Yamaguchi ^a & Richard S. Potember ^b

^a Mitsubishi Petrochemical Co. Ltd., Tsukuba Research Center, 8-3-1
Chuo, Ami, Inashiki, Ibaraki, 300-03, JAPAN

^b Johns Hopkins University, Applied Physics Laboratory, Laurel, MD,
20723, U.S.A.

Version of record first published: 24 Sep 2006.

To cite this article: Shoji Yamaguchi & Richard S. Potember (1995): STM Tip Induced Phase Transition of Copper Tetracyanoquinodimethane (CuTCNQ), Molecular Crystals and Liquid Crystals Science and Technology. Section A. Molecular Crystals and Liquid Crystals, 267:1, 241-248

To link to this article: <http://dx.doi.org/10.1080/10587259508034001>

PLEASE SCROLL DOWN FOR ARTICLE

Full terms and conditions of use: <http://www.tandfonline.com/page/terms-and-conditions>

This article may be used for research, teaching, and private study purposes. Any substantial or systematic reproduction, redistribution, reselling, loan, sub-licensing, systematic supply, or distribution in any form to anyone is expressly forbidden.

The publisher does not give any warranty express or implied or make any representation that the contents will be complete or accurate or up to date. The accuracy of any instructions, formulae, and drug doses should be independently verified with primary sources. The publisher shall not be liable for any loss, actions, claims, proceedings, demand, or costs or damages whatsoever or howsoever caused arising directly or indirectly in connection with or arising out of the use of this material.

STM TIP INDUCED PHASE TRANSITION OF COPPER TETRACYANOQUINODIMETHANE (CuTCNQ)

SHOJI YAMAGUCHI* AND RICHARD S. POTEMBER

*Mitsubishi Petrochemical Co. Ltd., Tsukuba Research Center

8-3-1 Chuo, Ami, Inashiki, Ibaraki 300-03, JAPAN

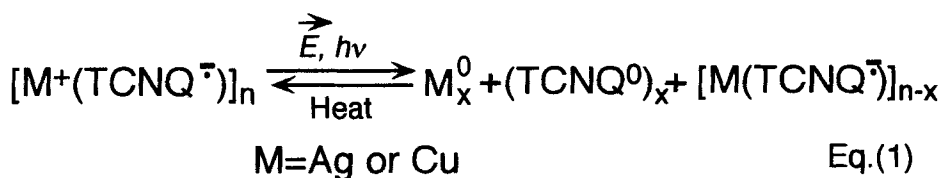
Johns Hopkins University, Applied Physics Laboratory,

Laurel, MD 20723, U.S.A.

Abstract We have demonstrated a field-induced, charge-transfer reaction driven by the electric field at the STM tip when the field generated by the STM exceeds the switching threshold of CuTCNQ charge transfer complex. We discuss the mechanism of this nanoscopic phenomenon in comparison with macroscopic observations.

INTRODUCTION

Silver and copper tetracyanoquinodimethane (TCNQ) salts show interesting electrical¹ and optical² field-induced phase transitions. The resistivity of these materials switches from a high impedance state to a low impedance state within a few nanoseconds by applying an electric field. The low impedance state can be switched back to the original high impedance state by the application of a sort current pulse or thermal heating. The optical properties of these materials are also switched by laser irradiation. The color of switched area changes to yellow (the color of neutral TCNQ) from unswitched green (CuTCNQ) or blue (AgTCNQ) color. The switched yellow spots can also be switched back to the original color by heating the spot with the defocused laser beam. In addition to TCNQ, TCNQ derivatives such as 2,3,5,6-tetrafluorotetracyanoquinodimethane (TCNQF₄)³; 11,11,12,12-tetracyano-2,6-naphtho-quinodimethane (TNAP)⁴; 2,5-dimethoxy-TCNQ and 2,5-dialkyl-TCNQ⁵ also show the same field-induced phase transition phenomenon. The mechanism of these phenomena has been proposed by Potember et al. from infrared, Raman, Auger, X-ray photoelectron spectroscopy as follows : ²



The above bulk property mechanism agrees with the results of both electrical and optical switching experiments on metal-TCNQ complexes. The production of neutral TCNQ in the 1:1 CuTCNQ complex is responsible for the mixed valence state. It is well known that the mixed valence complexes of TCNQ usually give higher conductivity than the corresponding fully charge-transferred complexes. The production of neutral TCNQ can change the optical properties as well. Our results do not support the report that the interface between the Al electrode and the rough solution-grown CuTCNQ surface plays a more important role for the switching of CuTCNQ.^{6,7}

We used the scanning tunneling microscopy (STM) to visualize surface structures of silver TCNQ at molecular level resolution.⁸ We found nanometer scale surface changes on silver TCNQ complexes during our study. In this study, we had some difficulty visualizing the unswitched states of silver TCNQ because of its poor conductivity. Therefore, we chose to examine copper complex of TCNQ because CuTCNQ is 1000 times more conductive than AgTCNQ in the unswitched high-impedance state.⁹ We have previously reported on an STM topographic study of the polycrystalline CuTCNQ⁸ and of the vacuum deposited CuTCNQ.¹⁰ We have also demonstrated a field-induced, charge-transfer reaction driven by the electric field at the STM tip when the field generated by the STM exceeds the switching threshold of the CuTCNQ charge-transfer complex.¹⁰ Similar observations have recently been reported for CuTCNQ thin films.¹¹ In this paper, we also discuss the STM tip field induced switching characteristics of CuTCNQ films in comparison with bulk electrical switching characteristics.

EXPERIMENTAL

TCNQ (98%, Aldrich) was purified by recrystallization from acetonitrile prior to use. Copper shot (99.9995%, 2-4 mm, Aldrich) was used as a deposition source without further purification. The Johns Hopkins dual-source vacuum deposition chamber was used for the preparation of CuTCNQ films. Background pressure was kept under 10^{-6} torr. The density of TCNQ used for a quartz crystal thickness monitor was 1.34 as measured by pycnometry. The copper and neutral TCNQ double-layered films were heated to 100°C for 1 minute to obtain green CuTCNQ films. Thin films of CuTCNQ were prepared on several substrates, including highly oriented pyrolytic graphite (HOPG, ZYA grade, Union Carbide), single crystal molybdenum disulfide (MoS₂, mined in Quebec) single crystal potassium chloride (KCl, Optvac) and mica (ASTM V2 grade, Asheville-Schoonmaker Mica Co.). HOPG, MoS₂, KCl and mica were cleaved in air prior to use and maintained at 293K for depositions in the vacuum chamber. Polycrystal-

line CuTCNQ and AgTCNQ were prepared on cleaned copper and silver plates (10 x 25 x 0.1 mm) in vials by a solution growth method.¹ The details of STM experimental conditions used in this study are described in our earlier papers.^{10,12} The constant current mode was used to record STM images. We modified a commercial STM(SA1-800, Park Scientific Instruments) to be able to use it in conjunction with an external pulse generator (Hewlett Packard 8116A pulse/function generator). We also modified the STM operational software to allow us to deliver a voltage pulse at a specific location on the sample. Local tunneling barrier height (dI/dZ) images were recorded simultaneously with regular STM images using an STM in conjunction with an external AC modulation source (Hewlett Packard 204C oscillator with 30dB 355D VHF attenuator) and a lock-in amplifier (EG&G Princeton Applied Research model 5210). The amplitude of the modulation signal was 3 mV ($\Delta s=0.24\text{\AA}$). The frequency of the modulation was 1.6 kHz. The STM scanning frequency in the barrier height mode was 0.25 - 1.0 Hz. The volume and surface resistivity was measured by a four-point probe resistivity technique (Mitsubishi Petrochemical, Loresta AP). Resistivity geometrical correction factors for finite samples were calculated based on the Yamashita's method¹³ and verified experimentally.¹⁴

RESULTS AND DISCUSSION

We require smooth films of CuTCNQ for our STM study. Atomically flat substrates, such as HOPG, MoS₂, mica and KCl provided a smooth surface for the STM study as well as a method to make ordered film structures. STM clearly showed some ordered film structures on HOPG, MoS₂ and KCl. HOPG gave grain sizes of 1-5 μm . MoS₂ gave grain sizes of 1-3 μm . KCl gave grain sizes of 1-2 μm . Mica did not produce films with ordered texture. STM requires samples and/or substrates with conductivity to maintain stable tunneling conditions. Among the above substrates, HOPG and MoS₂ are metallic conductors, whereas KCl and mica are electrical insulators. With KCl substrates, it was difficult to obtain stable tunneling conditions because it is insulating. MoS₂ substrates often gave us similar difficulties. In contrast to MoS₂, HOPG substrates always gave us stable tunneling conditions. The volume resistivity and the surface resistivity of HOPG was $1.1 \times 10^{-3} \Omega\cdot\text{cm}$ and $5.4 \times 10^{-3} \Omega/\square$ at room temperature, which is lower than that of a MoS₂ ($2.4 - 5.0 \times 10^{-1} \Omega\cdot\text{cm}$ and $3.0 - 5.0 \Omega/\square$). The resistivity of HOPG was very stable during measurements, whereas that of MoS₂ was not stable. MoS₂ is a natural mineral. It contains impurities and air voids between the layers. The contact resistance between the layers can not be ignored. HOPG is artificially synthesized graphite, it provide a good electrical contacts between the films and

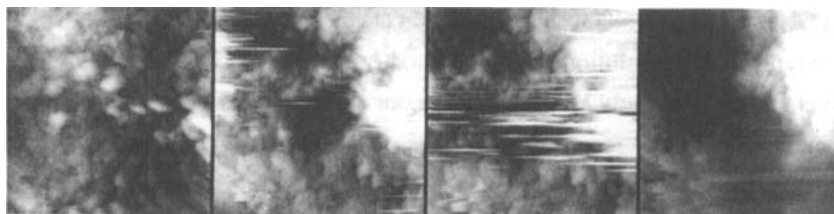


FIGURE 1 Subsequent images ($1 \times 1 \mu\text{m}$ scan size) of the continued phase transition of CuTCNQ on HOPG

STM. For these experiments, we chose HOPG substrates because of the stability of the STM imaging and HOPG made films with larger grain size of CuTCNQ.

The CuTCNQ films were sufficiently conductive to visualize the unswitched surface by the STM.⁸ When we imaged with tunneling voltages that exceeded the threshold of CuTCNQ, we saw field-induced phase transitions driven by the electric field produced at the STM tip to make 200-nanometer-sized domains. Subsequent images ($1 \times 1 \mu\text{m}$ scan size) shown in figure 1 revealed the continued phase transitions of CuTCNQ those were quite similar to the phase transitions of AgTCNQ.⁸ We could clearly observe the neutral reaction products of equation (1) segregate as a hole formed and white streaks appeared across the image. The white streaks were due to the formation of neutral copper and neutral TCNQ. The neutral TCNQ molecules were removed by the STM scans, because neutral TCNQ molecules are insulating. Only a very thin layer of neutral TCNQ molecules were permitted to stay on CuTCNQ surface by the operational mechanism of the STM. Dark hole regions were expanding due to the continued production of TCNQ[•] with time. This observation agrees with the phase transition mechanism that we described in equation (1). We observed the phase transition of CuTCNQ during STM scans.

We next used the modified STM system, described in the experimental section, to apply the electric field from the STM tip to induce the phase transition at the desired locations on CuTCNQ films. We first tested the pulse amplitude dependence on CuTCNQ films. Dark spots were found to occur when voltage pulses exceeded $\sim 3 \times 10^5$ V/cm.¹⁰ The size of dark spots varied from 100 nm to 500 nm. The depth of dark spots varied from 20 - 50 nm. In contrast, white hillocks appeared on CuTCNQ films when voltage pulses were approximately 1×10^5 V/cm and in the several hundred milliseconds range. The shape and size of hillock varied from 200 nm to $1 \mu\text{m}$ as shown in figure 2. The size and depth of the dark spots and white hillocks produced by the STM tip also varied depending on whether the tip was electrochemically etched or mechanically cut.

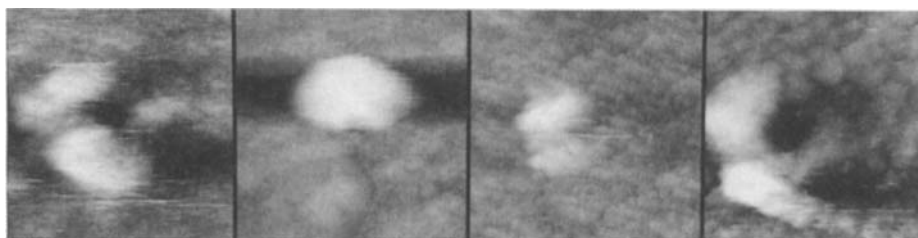


FIGURE 2 Various size and shape of white hillocks (200 nm to $1\mu\text{m}$) appeared on CuTCNQ films when voltage pulses were approximately 10^5 V/cm ($3 \times 3\mu\text{m}^2$)

Electrochemically etched tips were used for above experiments and gave reproducible results. Mechanically cut Pt/Ir tips were usually dull and had irregular profiles and spurs. Whereas, the Pt/Ir tips, fabricated by bulk etching and micro polishing 2 step electrochemical etching method had a very high aspect ratio (5° - 10° cone half angle) and a small radius of curvature ($\sim 50\text{nm}$).¹⁵ The tip geometry played an important role in STM surface modification experiments.

We concentrated our work on the white hillocks, because white hillocks appear to be the low impedance state of CuTCNQ. Under the constant current mode of the STM, more conductive parts were the brighter parts in the images. The STM tip does not need to approach the surface to maintain constant tunneling current on more conductive parts in comparison with less conductive parts. A +2V pulse with respect to the tip was applied to a 200 nm thick CuTCNQ film to give a $1\mu\text{m}$ diameter white hillock. Before we applied +2V pulse, we recorded the images over 5×5 , 3×3 , $1 \times 1\mu\text{m}^2$ areas. We only saw a rugged surface created by the +2V pulse on the next $1 \times 1\mu\text{m}^2$ scan, however, we saw a large white hillock on the subsequent 3×3 , $5 \times 5\mu\text{m}^2$ scans as shown in figure 3. This white hillock was very stable (for over 2 days) and it continued to give good quality STM images.

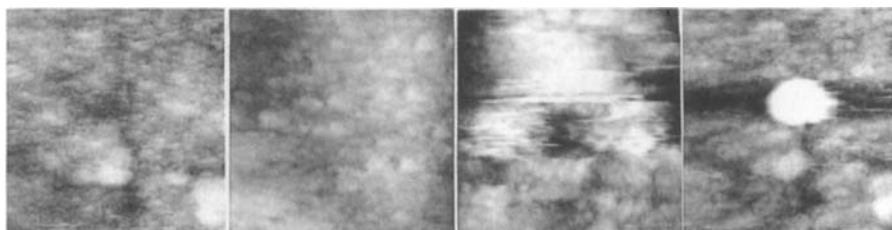


FIGURE 3 Topographic change of CuTCNQ film before and after +2V pulse (from left to right, before pulse 5×5 , $1 \times 1\mu\text{m}^2$, after pulse 1×1 , $5 \times 5\mu\text{m}^2$ scan, $V_t = 0.3\text{ V}$, $I_t = 2.8\text{ nA}$)

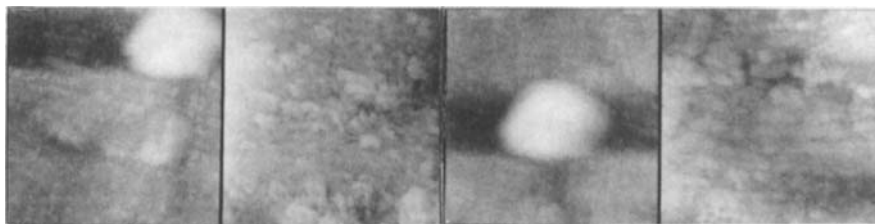


FIGURE 4 Topography of the switched parts and the unswitched parts (from left to right unswitched part 3×3 , 1×1 , switched part 3×3 , $1 \times 1 \mu\text{m}^2$, $V_t + 0.28 \text{ V}$, $I_t 2.8 \text{ nA}$)

A possible mechanism responsible for this white hillock formation is material transfer from a top of Pt/Ir tip, topographical upheaval by plastic deformation of films and increasing conductivity of CuTCNQ due to the phase transition according to equation (1). It was reported that a Au tip gave hillocks by field evaporation mechanism and the threshold for Au was 3.5–4.0 V.¹⁶ The evaporation field of field ion microscopy was also reported to be 404 MV/cm for Au, 786 MV/cm for Pt and 886 MV/cm for Ir.¹⁷ In our case for a Pt/Ir tip, a +2V pulse is unlikely to involve the field evaporation. Topography of the switched parts was quite similar to that of the unswitched parts as shown in figure 4. The switched white hillock region kept the original grain structure at the sub-micron scale even after the switching. We did not find any different species that came out from the STM tip (melt-dropped tip materials or contaminants) to produce hillock on the switched part of CuTCNQ surface.

When we recorded the I/V spectrum on the white hillock by scanning from negative bias voltage to positive bias voltage, we consistently found a decrease in the size of the hillock. When we applied the opposite polarity, but the same amplitude of the pulse voltage to the tip, we observed the dramatic morphological change shown in figure 5. We could clearly see the original surface between the separated white hillock after the

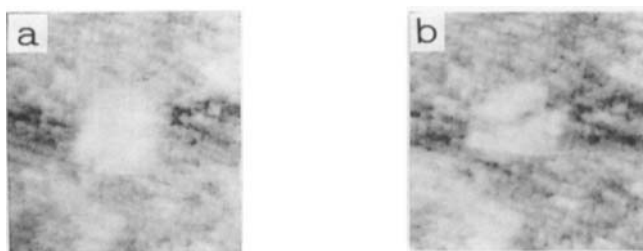


FIGURE 5 Morphology change of switched hillock on CuTCNQ by opposite polarity of first pulse (a) Before -2V pulse (left); (b) After -2V pulse (right) (Both scan size is $3 \times 3 \mu\text{m}$, $V_t = 0.28 \text{ V}$, $I_t = 4 \text{ nA}$).

application of the negative pulse. This indicated that the white hillocks were not produced simply by topographical upheavals. It should be possible to convert the entire spot back to the original state by optimizing the experimental conditions.

Binnig et al. reported that the gap modulation signal dI/dZ is proportional to the square root of the work function of the sample surface.¹⁸ It is called the local tunneling barrier height (dI/dZ) images. We took the dI/dZ images on the partially switched CuTCNQ film as shown in figure 6. This image clearly showed the reduction of the barrier height for the switched region (a white hillock), whereas the barrier height was nearly constant for the other regions including the large fissure on the upper right corner. Utsugi reported that the nanofeatures on Ag-Se films created by the STM etching technique gave quite uniform dI/dZ image even though the topographic image in the same area had two grooves on the surface. He concluded that his modified surface was chemically homogeneous.¹⁹ The difference of the local tunneling barrier height between the switched part and the unswitched part indicates that the chemical composition is different, we did not see any topographical difference between the switched part and the unswitched part as shown in figure 4 and we did not have any contact upper electrodes in STM switching experiments. From this evidence, we conclude that the white hillocks produced by STM pulsing were of the low impedance state of CuTCNQ. This demonstrates that the electric switching phenomena of metal-TCNQ is not an interfacial phenomena but a bulk property of metal-TCNQ at least at nanoscopic scale.

We also examined macroscopic switching for CuTCNQ and AgTCNQ without a top Al electrode. We grew polycrystalline CuTCNQ on Cu foils and AgTCNQ on Ag foils. We used a gold-plated beryllium copper spring-loaded contact probe (0.5 mm diameter, round top) as a upper electrode and Cu and Ag foil as a bottom electrode for

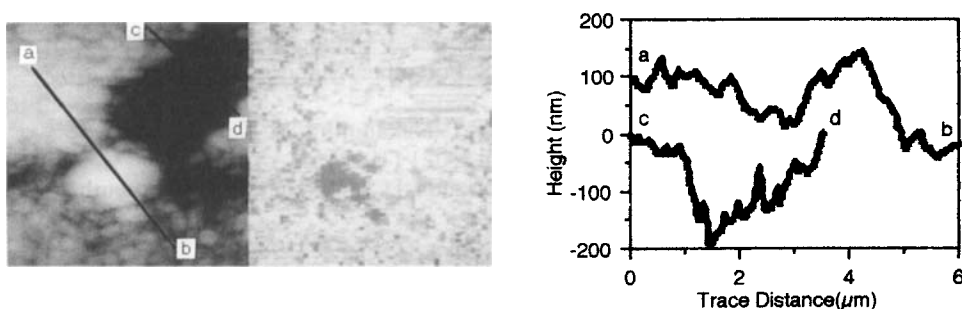


FIGURE 6 Topographic image (left, $7 \times 7 \mu\text{m}^2$, $V_t +0.29\text{V}$, $I_t 1.0 \text{ nA}$), dI/dZ images (center) on the partially switched CuTCNQ film, Cross sectional views along the indicated lines on the topographic image (right)

Cu-CuTCNQ-Au and Ag-AgTCNQ-Au switching devices. These devices exhibited non-linear switching in the range of 6-9 volts and produced the neutral TCNQ with visible yellow spots around the contact probe at more than 20V. These macroscopic observations were quite similar to the STM nanoscopic observations. Hoagland et al. proposed an Al/CuTCNQ interface mechanism for the metal TCNQ switching phenomena.⁷ Our STM switching experiments and contact probe switching experiments did not support this interface mechanism. Our results support the bulk property mechanism shown in the equation (1).

ACKNOWLEDGMENT

We gratefully acknowledge the support of the U.S. Department of the Navy. We wish to thank C.A. Viands for her assistance, C. A. Valenzuela for modifying STM software.

REFERENCES

1. R. S. Potember, T. O. Poehler and D. O. Cowan, Appl. Phys. Lett., **34**, 405 (1979)
2. R. S. Potember, T. O. Poehler and R. C. Benson, Appl. Phys. Lett., **41**, 548 (1982)
3. R. S. Potember, T. O. Poehler, A. Rappa, D. O. Cowan and A. N. Bloch, Synth. Met., **4**, 371 (1982)
4. R. S. Potember, T. O. Poehler, A. Rappa, D. O. Cowan and A. N. Bloch, J. Am. Chem. Soc., **102**, 3659 (1980)
5. R. S. Potember, T. O. Poehler, D. O. Cowan, F. L. Carter and P. Brant, Molecular Electronic Devices, ed. by F. L. Carter (Marcel Dekker, NY), 73 (1983)
6. C. Sato, S. Wakamatsu, K. Tadokoro and K. Ishii, J. Appl. Phys., **68**, 6535 (1990)
7. J. J. Hoagland, X. D. Wang and K. W. Hipps, Chem. Mater., **5**, 54 (1993)
8. S. Yamaguchi, C.A. Viands and R.S. Potember, J. Vac. Sci. Technol., **B9**, 1129 (1991)
9. W. J. Siemons, P. E. Bierstedt and R. G. Kepler, J. Chem. Phys., **39**, 3523 (1963)
10. S. Yamaguchi, C. A. Valenzuela and R. S. Potember, Mat. Res. Soc. Symp. Proc., Vol. 276, 265 (1992)
11. M. Matsumoto, Y. Nishio, H. Tachikbana, T. Nakanmura, Y. Kawabata, H. Samura and T. Nagamura, Chem. Lett., **1021** (1991)
12. S. Yamaguchi, T.J. Kistenmacher, C.A. Viands, H.S.-W. Hu and R.S. Potember, Synth. Met., **63**, 61 (1994)
13. M. Yamashita and M. Agu, Jpn. J. Appl. Phys., **23**, 1499 (1984)
14. M. Yamashita, S. Yamaguchi, and H. Enjoji, Jpn. J. Appl. Phys., **27**, 869 (1988)
15. I. H. Musselman and P. E. Russell, J. Vac. Sci. Technol., **A8**, 3558 (1990)
16. H. J. Mamin, S. Chiang, H. Birk, P. H. Guethner and D. Rugar, J. Vac. Sci. Technol., **B9**, 1398 (1991)
17. W. Müller and T. T. Tsong, Field Ion Microscopy (Elsevier, New York, 1969), p58
18. G. Binnig and H. Rohler, Surf. Sci., **126**, 236 (1983)
19. Y. Utsugi, Jpn. J. Appl. Phys., **32**, 2969 (1993)